



ELSEVIER

Contents lists available at ScienceDirect

International Journal of Heat and Mass Transfer

journal homepage: www.elsevier.com/locate/hmt

Reexamination of electron-phonon coupling constant in continuum model by comparison with Boltzmann transport theory

Wuli Miao, Moran Wang*

Key Laboratory for Thermal Science and Power Engineering of Ministry of Education, Department of Engineering Mechanics and CNMM, Tsinghua University, Beijing 100084, China

ARTICLE INFO

Article history:

Received 9 November 2020

Revised 24 February 2021

Accepted 27 March 2021

Keywords:

Heat conduction

Electron-phonon coupling

Two-temperature model

Non-equilibrium effect

ABSTRACT

The electron-phonon (e-ph) coupling process in ultrafast dynamics involves non-equilibrium effects including non-thermalized electrons and temporal non-equilibrium between different phonon branches. During such process, the two-temperature model (TTM) is employed to extract the relevant e-ph coupling constant though experiments themselves have demonstrated the invalidity of TTM. In this work, through fitting the results of Boltzmann transport theory by that of TTM, we quantitatively investigate the influence of the non-equilibrium effects on extraction of the e-ph coupling constant in TTM. The extracted e-ph coupling constant will be indeed underestimated yet not significantly by about 7% under the influence of non-equilibrium between different phonon branches for Au, Ag. Additionally, when the excitation pulse width is comparable to the e-ph relaxation time of electrons, non-thermalized electrons exists after excitation and thus the extracted e-ph coupling constant in TTM shows over 20% deviation. Therefore, the excitation pulse width is required to be larger than 300 fs and 500 fs for Au, Ag, respectively at room temperature if the error is controlled within 10%. This work will provide insightful indication for the measurement of the e-ph coupling constant in femtosecond pump-probe experiments.

© 2021 Elsevier Ltd. All rights reserved.

1. Introduction

Electron-phonon (e-ph) coupling plays a crucial role in determining the fundamental physical properties such as thermal conductivity, carrier mobility, relaxation rate for energy conversion facilities and semiconductor electronic devices [1,2]. Thus, energy exchange through e-ph coupling draws increasing attention. In femtosecond pump-probe experiments and Raman Spectroscopy, electrons and phonons are demonstrated with distinct temperatures so that the energy transfer between each other is significant [3,4]. In order to describe the strength of energy exchange in metals, the e-ph coupling constant defined as energy transfer rate per unit volume and per temperature difference between electrons and phonons is quantitatively introduced [5]. A thorough understanding and clarification of the e-ph coupling constant is urgent.

In early time, through simplifying the original e-ph scattering term in the Boltzmann transport equation, the e-ph coupling constant was formulated for the free electron model [6]. After nearly 30 years, Allen insightfully established the relationship between coupling function and Eliashberg function in superconductivity, and then derived the prevailing theoretic formula of the e-ph

coupling constant which became a basic principle for most metals [7]. Thus, combined with *ab initio* calculation or experimental results of Eliashberg function, the e-ph coupling constant can be obtained by the application of Allen's theoretic formula [8]. Moreover, the e-ph coupling constant can also be directly computed from the original e-ph scattering term by *ab initio* method developed over the past decade [9–11]. These predictions are all based on the quasi-equilibrium assumption for electrons and phonons subsystems respectively. On the other hand, the direct measurement of the e-ph coupling constant by ultrafast pump-probe experiments provides an alternative choice [12,13]. In ultrafast pump-probe experiments, a pump laser is firstly irradiated on the metal surface. After a delay time, a probe laser is incident to detect the reflectance change of the metal surface which is related to electron and phonon temperature changes [14,15]. Afterwards, the two-temperature model (TTM) is adopted where electrons and phonons are assigned with different temperatures and then related by an e-ph coupling constant [5]. Through fitting the normalized probe signal of reflectance change by the TTM, an e-ph coupling constant is correspondingly extracted [16,17]. However, many researchers have demonstrated that the application of the TTM in ultrafast pump-probe experiments is questionable due to significant non-equilibrium effects including non-thermalized electrons and temporal non-equilibrium between different phonon branches [18–24].

* Corresponding author.

E-mail addresses: mrwang@tsinghua.edu.cn, moralwang@gmail.com (M. Wang).

The relaxation time of electron-electron (e-e) interaction is comparable to or even larger than that of e-ph interaction so that electrons are not able to scatter with each other frequently [18,19,25]. Thus, e-ph scattering is significant to restore equilibrium and a large amount of thermal energy has been transferred to phonons before electrons thermalize [21,26]. If the time scale for the excitation of electrons is comparable to the relevant relaxation time including not only the e-e scattering time but also the e-ph scattering time, electrons are non-thermalized after excitation. In addition, non-equilibrium between different phonon branches also occurs due to the different coupling strength between electrons and different phonon branches [23,24,27]. These non-equilibrium effects will indeed influence the e-ph coupling process and the Boltzmann transport theory is more appropriate to capture these influences in pump-probe experiments [25,28,29]. In contrast, the continuum TTM model as the simplest expression of coupling between electrons and phonons is widely employed. As a result, the e-ph coupling constant extracted still using the TTM would be affected. A more consistent second moment of Eliashberg function was displayed for cuprate superconductors by the application of Boltzmann transport theory rather than TTM [30]. One recent experiment has shown that the TTM can still yield a consistent value of second moment of Eliashberg function once experimental data are analyzed at time delays when electrons with temperature determined by measurement are already quasi-equilibrium [21]. It still remains to re-examine how much these non-equilibrium effects will influence the extracted e-ph coupling constant using the TTM.

As experiments themselves are complicated and hard to distinguish the different influence of non-equilibrium effects, the coupled electron and phonon Boltzmann transport equations (BTEs) with the form of relaxation time approximation scattering term is further adopted for comparison [31]. A normalized parameter, including the effect from electron and phonon temperature changes, is employed for quantitative comparison. The TTM is a continuum model based on the quasi-equilibrium assumption whereas the BTEs directly deal with the distribution function and include the non-equilibrium effects. Once the solution of the BTEs is obtained, the e-ph coupling constant in the TTM is correspondingly extracted through fitting the normalized parameter of the BTEs by that of the TTM. This extraction includes the influence of non-equilibrium effects, and thus the quantitative estimation could be made. The remaining of this article is organized as below: a brief introduction of the coupled electron and phonon BTEs and the TTM are shown in Section 2; through fitting the normalized parameter of the BTEs by that of the TTM, the extracted e-ph coupling constant in the TTM is analyzed and the influence of non-thermalized electrons and temporal non-equilibrium between different phonon branches on which is further checked in Section 3, respectively; concluding remarks are finally made in Section 4.

2. Boltzmann transport theory and continuum model

2.1. Boltzmann transport equation

The intensity form of the coupled electron and phonon BTEs is formulated as [27,31]

$$\frac{\partial I_{\varepsilon}}{\partial t} + \mathbf{v}_e \cdot \nabla_{\mathbf{r}} I_{\varepsilon} = -\frac{I_{\varepsilon} - I_{\varepsilon}^{eq}(\tilde{T}_e)}{\tau_{e-ph}(\varepsilon)} + S_{\text{BTE}}(\mathbf{r}, t), \quad (1)$$

$$\frac{\partial \phi_{\omega,p}}{\partial t} + \mathbf{v}_{ph,p} \cdot \nabla_{\mathbf{r}} \phi_{\omega,p} = -\frac{\phi_{\omega,p} - \phi_{\omega,p}^{eq}(\tilde{T}_e)}{\tau_{ph-e}(\omega, p)} - \frac{\phi_{\omega,p} - \phi_{\omega,p}^{eq}(\tilde{T}_{ph})}{\tau_{U,ph-ph}(\omega, p)}, \quad (2)$$

where I_{ε} and $\phi_{\omega,p}$ are the electron and phonon intensity respectively with ε the electron energy, ω the phonon frequency and p the different branch including the transverse acoustic (TA) and longitudinal acoustic (LA) phonons. The e-e interaction is neglected in formulating the scattering term of electrons due to both the greatly restricted scattering phase space by Pauli exclusion principle under low fluence excitation and screen effect [1,19,25,32]. S_{BTE} denotes the flux of pump pulse energy absorbed by electrons. \tilde{T}_e and \tilde{T}_{ph} are the local pseudo-temperature of electrons and phonons determined by the energy conservation principle during the e-ph collision and the phonon-phonon (ph-ph) collision process separately.

The energy-dependent e-ph relaxation time and the frequency-dependent ph-e relaxation time are expressed respectively as [31]:

$$\frac{1}{\tau_{e-ph}(\varepsilon)} = 2\pi \sum_{\mathbf{p}} \int \{ [n_{\omega}^{eq}(\tilde{T}_{ph}) + 1 - f_{\varepsilon-\hbar\omega}^{eq}(\tilde{T}_e)] C_{e-ph}(\varepsilon, \varepsilon - \hbar\omega, \omega, \mathbf{p}) + [n_{\omega}^{eq}(\tilde{T}_{ph}) + f_{\varepsilon+\hbar\omega}^{eq}(\tilde{T}_e)] C_{e-ph}(\varepsilon, \varepsilon + \hbar\omega, \omega, \mathbf{p}) \} d\omega, \quad (3)$$

$$\frac{1}{\tau_{ph-e}(\omega, p)} = 2\pi \int \frac{D_e(\varepsilon)}{D_{ph}(\omega, p)} [f_{\varepsilon}^{eq}(\tilde{T}_e) - f_{\varepsilon+\hbar\omega}^{eq}(\tilde{T}_e)] \times C_{e-ph}(\varepsilon, \varepsilon + \hbar\omega, \omega, \mathbf{p}) d\varepsilon. \quad (4)$$

The coupling function C_{e-ph} in Eqs. (3) and (4) is further related to the Eliashberg function $\alpha^2 F(\omega, p)$ through $C_{e-ph} \simeq \sqrt{\varepsilon_F/\varepsilon} \alpha^2 F(\omega, p)$. The free electron band structure with the density of states $D_e(\varepsilon)$ and the power law expression of the phonon dispersion relation along [0 0 1] direction with the branch-dependent density of states $D_{ph}(\omega, p)$ are used [31]. Additionally, the ph-ph relaxation time is approximated directly by the empirical relation as $1/\tau_{U,ph-ph}(\omega, p, \tilde{T}_{ph}) = B_U \omega^2 \tilde{T}_{ph} \exp(-\Theta_p/3\tilde{T}_{ph})$ with the input parameters also found in Ref. [31]. For the numerical solution, the discrete-ordinate-method (DOM) is applied where an implicit and first-order upwind scheme is used for the temporal and spatial discretization [31,33]. Besides, the Gauss-Legendre (G-L) quadrature is adopted for the numerical integration over the electron energy, the phonon frequency and the angular variable due to its high efficiency [34].

2.2. Two-temperature model

The TTM widely adopted for the description of the coupled electron and phonon transport process is written as [5,35]

$$c_e(T_e) \frac{\partial T_e}{\partial t} = \nabla \cdot (\kappa_{eq}(T_e, T_{ph}) \nabla T_e) - G(T_e - T_{ph}) + S_{\text{TTM}}(\mathbf{r}, t) \quad (5)$$

$$c_{ph} \frac{\partial T_{ph}}{\partial t} = \nabla \cdot (\kappa_{ph} \nabla T_{ph}) + G(T_e - T_{ph}) \quad (6)$$

where T_e and T_{ph} are the local electron and phonon temperature respectively. The temperature-dependent electronic heat capacity $c_e(T_e) = \int_{\text{Fermi}} (\varepsilon - \varepsilon_F) \frac{d f_{\varepsilon}^{eq}}{d T_e} D_e(\varepsilon) d\varepsilon$ are calculated consistently provided the electron band structure in the BTEs is given [31]. The phonon heat capacity $c_{ph} = \sum_{\mathbf{p}} \int_0^{\omega_{\text{max},p}} \hbar \omega \frac{d n_{\omega}^{eq}}{d T_e} D_{ph}(\omega, p) d\omega$

is nearly constant and is $2.465 \times 10^6 \text{ J}/(\text{m}^3\text{K})$, $2.499 \times 10^6 \text{ J}/(\text{m}^3\text{K})$ for Ag, Au respectively as the temperature change of phonon is relatively small. The effective electron thermal conductivity is modified as $\kappa_{eq}(T_e, T_{ph}) = \kappa_e T_e / T_{ph}$ with κ_e the commonly used electron thermal conductivity in the bulk material [35]. In the present work, κ_e is adopted to be $404.94 \text{ W}/\text{m}/\text{K}$, $326.88 \text{ W}/\text{m}/\text{K}$ for Ag, Au separately, which is also referred from Ref. [31], consistently. κ_{ph} is the phonon thermal conductivity whereas the diffusion of phonons is further neglected since the conductivity of phonons is far smaller than that of electrons in most metals [11]. Correspondingly, the drift term in phonon BTE (2) is ignored. S_{TTM} denotes the pump pulse energy absorbed by electrons. The e-ph coupling constant G relates energy exchange between electrons and phonons.

3. Results and discussion

In this Section, we consider the ultrafast dynamics for Au, Ag as the first step. Under the influence of temporal non-equilibrium between different phonon branches as well as non-thermalized electrons, the extracted e-ph coupling constant using the TTM is checked in Sub-section 3.1 and 3.2, respectively.

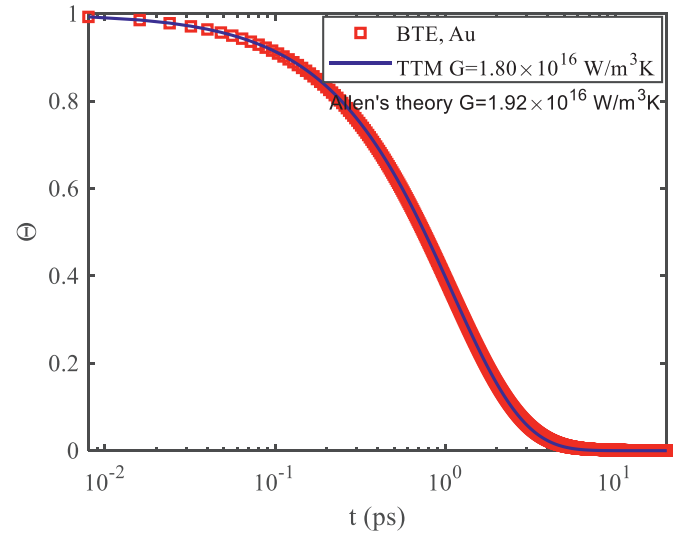
3.1. Influence of temporal non-equilibrium between different phonon branches

First of all, the drift term in electron BTE (1) and the diffusion of electrons in Eq. (5) is neglected for simplicity, which is commonly adopted in many experiments [14,16]. In order to intuitively investigate the influence of non-equilibrium between different phonon branches, the pump pulse energy irradiated on electrons sub-systems is not explicitly considered whereas it is manifested by a higher energy state in the initial condition [20]. Thus, the initial condition is set that electrons are assumed in equilibrium at 320 K with phonon undisturbed at room temperature (300 K) as a first step. For the fitting process, the normalized parameter is adopted

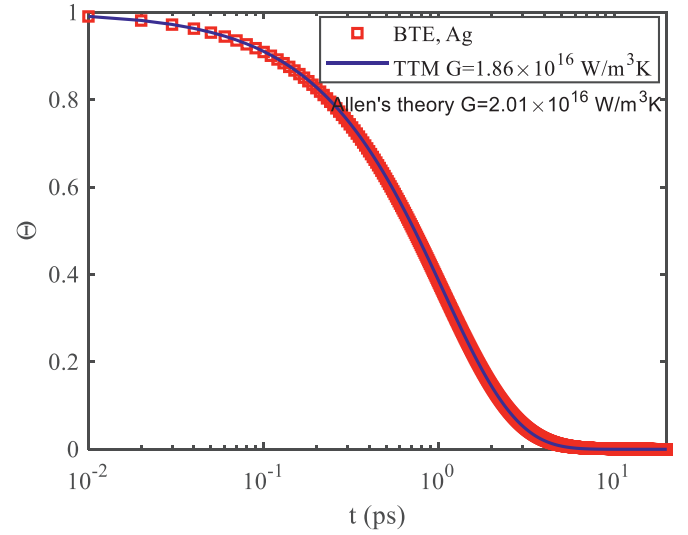
$$\Theta = \frac{a\Delta T_e + b\Delta T_{ph} - (a\Delta T_e + b\Delta T_{ph})_{\min}}{(a\Delta T_e + b\Delta T_{ph})_{\max} - (a\Delta T_e + b\Delta T_{ph})_{\min}} \quad (7)$$

as fitting index. This expression is directly referred from the normalized reflectance change in ultrafast pump-probe experiments [14]. It describes that changes in both electron and phonon temperature might give rise to the reflectance change with the proportionality coefficient a and b , respectively, under the linear response approximation. Thus, the relevant temperature change cannot be up to several hundred Kelvins and the temperature difference of 20 K between electrons and phonons is set for the initial condition in the present work [15]. For another, when the temperature is higher than 1000 K, the excitation of d band electrons will make the e-ph coupling constant further temperature-dependent [36]. In contrast, for the temperature range in the present work, the e-ph coupling constant is temperature-independent. Usually, the ratio a/b is determined by fitting the measured normalized reflectance change with the TTM in experiments, which may be influenced by probe laser wavelength and materials [14]. However, in the present work, the value of a/b needs to be pre-given for the BTEs, and then the normalized parameter Θ of the BTEs can be calculated. Afterwards, the e-ph coupling constant in the TTM is extracted through fitting the normalized parameter Θ of the BTEs by that of the TTM via least-square method.

The choice of a/b is referred from different experimental condition and theoretical indication, and we set it to infinity with $a = 1$ and $b = 0$ for Au, Ag [14,37,38]. It is widely accepted that the contribution of the electron temperature change to the reflectance change is definitely dominant so that the phonon contribution can be nearly neglected for Au, Ag. Thus, the reduced form of Eq. (7) is $\Theta = \frac{\Delta T_e - (\Delta T_e)_{\min}}{(\Delta T_e)_{\max} - (\Delta T_e)_{\min}}$. The angular and spatial variables vanish in this case due to the negligible treatment of the drift term. The discretization of the electron energy and phonon spectrum is based on the abscissas of the G-L quadrature that are applied with 96 and 80 points for electrons and phonons, respectively. The fitting period is chosen that the electrons and phonons have nearly reached equilibrium at final state, and then set as 20 ps for both Au, Ag. The normalized parameter fitted by the TTM and the result of the extracted e-ph coupling constant are displayed in Fig. 1. Furthermore, the quantitative assessment of this extracted value is estimated by comparison with the theoretical value of Allen's formula as it represents the intrinsic property of materi-



(a)



(b)

Fig. 1. The fitting curve of the normalized parameter Θ and the extracted e-ph coupling constant considering the influence of temporal non-equilibrium between different phonon branches: (a) for Au; (b) for Ag. The red squares represent the normalized parameter of the BTEs whereas the blue line denotes that of the TTM with an extracted e-ph coupling constant. (For interpretation of the references to color in this figure legend, the reader is referred to the web version of this article.)

als. Allen's theory gives that $G = 3\hbar \int_{\text{Fermi window}} (\varepsilon - \varepsilon_F) \frac{d\varepsilon^{eq}}{dT} D_e(\varepsilon) d\varepsilon \times$

$\sum_p 2 \int_0^{\omega_{\max,p}} \frac{\alpha^2 F(\omega,p)}{\omega} \omega^2 d\omega / (\pi k_B T)$ with the Eliashberg function $\alpha^2 F(\omega, p)$ referred from our recent work [31]. As a result, the calculated e-ph coupling constant is $1.92 \times 10^{16} \text{ W}/(\text{m}^3\text{K})$, $2.01 \times 10^{16} \text{ W}/(\text{m}^3\text{K})$ for Au, Ag, respectively.

The e-ph coupling constant calculated by the BTEs is not a simple constant but displays rapid reduction by the influence of non-equilibrium between different phonon branches [31]. Thus, the investigation of this reduction on the extracted e-ph coupling constant in the TTM is an equivalent way to check the influence of this temporal non-equilibrium. The extracted e-ph coupling constant is

Table 1

The value of reflectivity (R) and optical penetration depth (δ) at the pump wavelength of 400 nm and 800 nm separately for Au, Ag.

Wavelength	400 nm		800 nm	
	R	δ/nm	R	δ/nm
Au	0.371	16.4	0.98675	12.9
Ag	0.848	16.3	0.9577	12.1

nearly 6%, 7% lower than that of Allen's theory for Au, Ag respectively. This result makes sense since the non-equilibrium between different phonon branches manifested by the reduction of the e-ph coupling constant in the BTEs will slow down the rate of reaching equilibrium between electrons and phonons. Thus, the overall e-ph coupling constant in the TTM is slightly underestimated when fitting with the BTEs. However, the influence of this reduction on the extraction is not explicitly significant. It might be attributed to that electrons and phonons almost tend to be equilibrium with only little temperature difference between each other when the e-ph coupling constant calculated by BTEs reduces to half of that from Allen's theory. In other words, the dominance role of the e-ph coupling constant lies in the initial stage of rapid energy transfer where the e-ph coupling constant in the BTEs is nearly consistent with that from Allen's theory. Correspondingly, the extracted e-ph coupling constant in the TTM is close to that of Allen's theory. Therefore, the extraction of the e-ph coupling constant in the TTM will be indeed underestimated yet not significantly by the influence of the temporal non-equilibrium between different phonon branches.

3.2. Influence of non-thermalized electrons

In this subsection, the irradiation energy of pump laser is explicitly considered, which can be treated as a source term. The drift term in electron BTE (1) and the diffusion of electrons in the TTM are also considered. The expression of this source term for the TTM is written as [17]:

$$S_{\text{TTM}}(z, t) = \sqrt{\frac{4\ln 2}{\pi}} \frac{(1-R)J}{t_p \delta} \exp\left(-\frac{z}{\delta} - 4\ln 2 \left(\frac{t-2t_p}{t_p}\right)^2\right). \quad (8)$$

In Eq. (8), J is the pump laser fluence. t_p is the full width at half maximum duration of the pump laser pulse and we term it as the excitation pulse width in short in the present work. R is the reflectivity of the metal and δ is the optical penetration depth, which are both dependent on the pump laser wavelength. The value of R and δ are referred from the optical properties, and then shown in Table 1 at the pump wavelength of 400 nm and 800 nm separately for Au, Ag [39].

The source term for the intensity form of the BTEs is written as:

$$S_{\text{BTE}}(z, t) = v_e \sqrt{\frac{4\ln 2}{\pi}} \frac{(1-R)J}{t_p \delta} \exp\left(-\frac{z}{\delta} - 4\ln 2 \left(\frac{t-2t_p}{t_p}\right)^2\right) \times \frac{1}{(\varepsilon_{\text{high}} - \varepsilon_{\text{low}})4\pi}, \quad (9)$$

which is directly referred from that of the TTM. ε_{low} and $\varepsilon_{\text{high}}$ are the lower limit and upper limit of the Fermi window, respectively. The more appropriate expression of the source term for the BTEs, describing the states after electrons absorb the irradiation energy, needs further attention. Due to the requirement of not too high temperature change by the linear response, the pump laser fluence is set to be smaller than 0.05 J/m² for all cases. Within the linear response regime, the change in the pump laser fluence has

nearly no effect on the extraction result. It also agrees with the recent experimental investigation that the second moment of Eliashberg function extracted from the femtosecond broadband optical spectroscopy is independent of the excitation fluence [21]. The actual value of t_p irradiated on the metal surface is larger than that initially ejected from the pump laser due to the broadening effect from the electro-optic modulator [40]. The expression of the source term in the TTM might describe the restored states around Fermi surface after the incidence of the pump laser since the complex electron-photon and e-e interaction are not explicitly considered. Thus, the value of t_p in the TTM is also a fitting parameter determined by fitting the rising stage of the measured normalized reflectance change, and then might be larger than the actual one irradiated on the metal surface [40]. Therefore, in the ultrafast pump-probe experiments, the value of t_p , a/b and e-ph coupling constant G are all fitting parameters, among which the a/b and the G jointly influence the falling stage and the following gradual period of the normalized index. In contrast, for fitting the normalized index Θ of the BTEs by that of the TTM in the present work, the value of t_p and a/b in the BTEs needs to be pre-given. The choice of a/b for Au, Ag is nearly clear and set to infinity as mentioned in the former sub-section. In comparison, the value of t_p in the source term depends on different experimental setup and is usually not given clearly in experiments. Thus, the different setup of t_p in the source term can be further checked in the present work.

Electrons and phonons are in room temperature for the initial condition and the boundary condition is set that the top and bottom surface of the metal film are both adiabatic. Thus, the thickness of the metal film is appropriately large to satisfy that heat has not yet been transferred to the bottom of the metal in the concerned fitting period. The length of 2200 nm, 2000 nm is set for Ag, Au respectively in the fitting period of 12 ps. Otherwise, interface transport needs to be considered where the coupling between electrons in metal and phonons in semiconductor substrate is still elusive [41,42]. In the DOM scheme, the number of abscissas of the G-L quadrature is chosen as 48 points for both the electron energy and phonon spectrum, and 32 points for the discretization of polar angle. Once the normalized index Θ of the BTEs is obtained, its maximum is shifted to be located at time $t = 0$. Afterwards, the value of a/b and t_p in the TTM is obtained by fitting the normalized index Θ . These values are found to be the same with that in the BTEs. Thus, the e-ph coupling constant is extracted by the least square method.

The fitting curve of the normalized index Θ and the extracted e-ph coupling constant are shown in Fig. 2 at the pulse width of 100 fs and 500 fs for both Au and Ag. The rapid rising stage mainly represents the excitation of electrons by absorbing the irradiation energy, during which the energy transfer from electrons to phonons also occurs. This physical picture also agrees with the experimental investigation and the theoretical analysis that the energy transfer through e-ph coupling is important before the thermalization of electrons [21,26]. Subsequently, the energy exchange between electrons and phonons dominates in the falling period until equilibrium is nearly reached between each other, then followed by the energy transport through the material. The overall trend of the normalized parameter of the TTM exhibits good consistency with that of the BTEs. However, in terms of the e-ph coupling constant, a large discrepancy between the extracted value and Allen's theoretical value exists for Au, Ag at the excitation pulse width t_p of 100 fs, whereas they agree with each other well at t_p of 500 fs. Furthermore, the extracted e-ph coupling constant at other pulse width as well as the relative error is displayed in Fig. 3.

Generally, this extracted e-ph coupling constant shows larger deviation from Allen's theory when the pulse width is smaller than 300 fs. The average e-ph relaxation time of electrons is 33.6 fs and

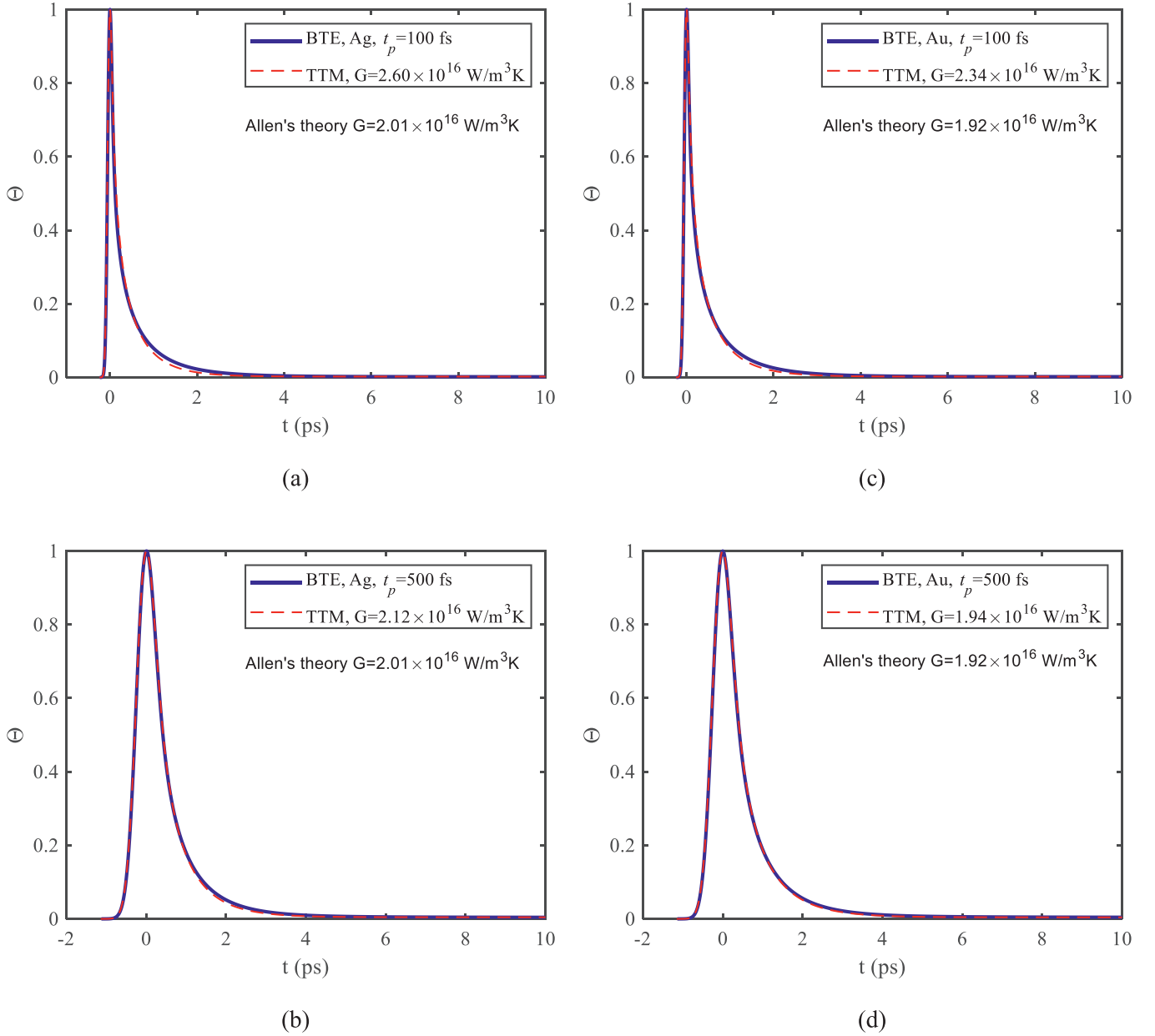


Fig. 2. The fitting curve of the normalized parameter Θ and the extracted e-ph coupling constant at pump pulse wavelength 400 nm considering the influence of non-thermalized electrons: (a) for Ag, $t_p = 100$ fs; (b) for Ag, $t_p = 500$ fs; (c) for Au, $t_p = 100$ fs; (d) for Au, $t_p = 500$ fs. The pump laser fluence is set to be 0.05 J/m², 0.01 J/m² for Ag, Au, respectively. The time step is adopted to be 6 fs, 15 fs at t_p of 100 fs, 500 fs, separately. The blue solid line represents the normalized parameter of the BTEs whereas the red dashed line denotes that of the TTM with an extracted e-ph coupling constant. (For interpretation of the references to color in this figure legend, the reader is referred to the web version of this article.)

26.9 fs for Ag and Au respectively at room temperature [31]. During the excitation period, the absorption of the incident radiation energy pushes electrons away from equilibrium and then the interaction with phonons helps to return to equilibrium. When the excitation pulse width is comparable to or a slightly larger than the e-ph relaxation time like the case of t_p smaller than 300 fs, electrons are not fully able to interact with phonons so that non-thermalized electrons exist after excitation. In contrast, if the pulse width is larger enough than the e-ph relaxation time like the case of t_p larger than 500 fs, the interaction between electrons and phonons is sufficient and thus electrons are almost thermalized after excitation. However, under the quasi-equilibrium assumption of the TTM, electrons are instantaneously thermalized, then followed by the standard e-ph energy exchange during the excitation process. Actually, due to the insufficient interaction between elec-

trons and phonons during the excitation process, electrons have higher thermal energy than that predicted by the TTM. When the normalization is further performed as Eq. (7), the maximum temperature change in the denominator for the BTEs is higher. Thus, the normalized parameter for the BTEs will be reduced and the TTM with a higher e-ph coupling constant may fit well. As a result, the extracted e-ph coupling constant in the TTM shows nearly over 20% overestimation compared with Allen's theory. Therefore, if we want to control the fitting error within 10%, the excitation pulse width is required to be larger than 300 fs and 500 fs for Au, Ag, respectively at room temperature. When the temperature is lower, the restriction on the excitation pulse width is stricter as the intrinsic e-ph relaxation rate is weakened. Although the temporal non-equilibrium between different phonon branches exists in these cases, it has a weak influence on the extraction com-

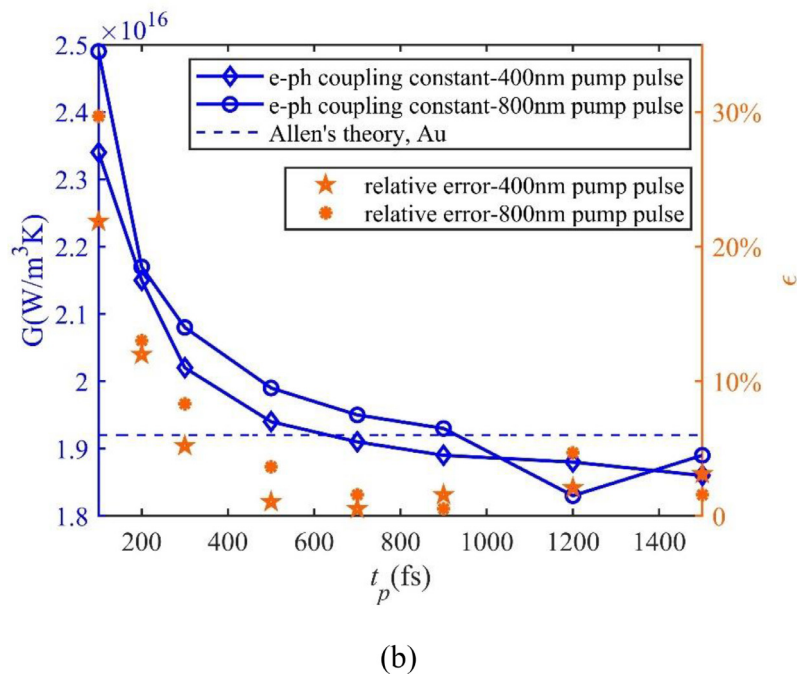
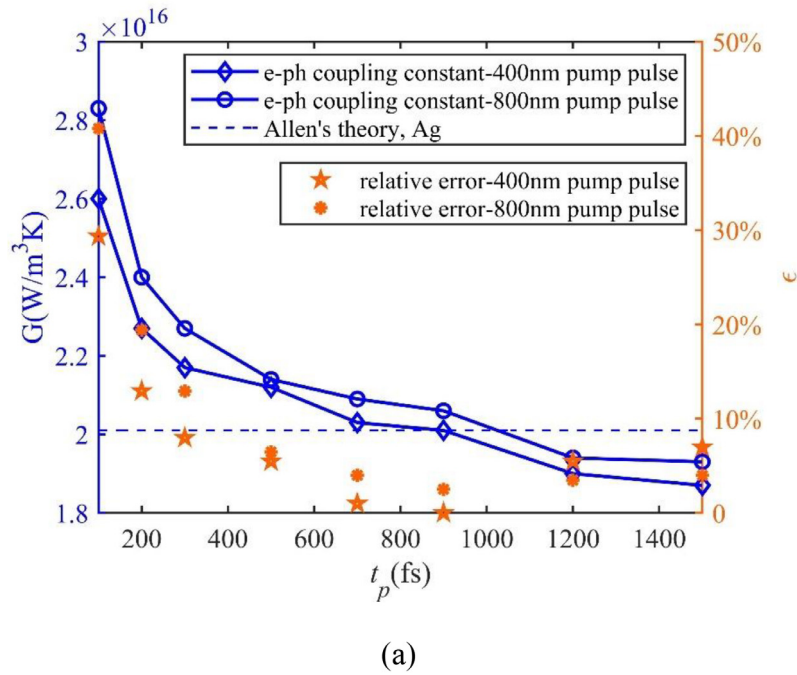


Fig. 3. The extracted e-ph coupling constant at different pulse width for both 400 nm and 800 nm pump wavelength and the relative error between this extracted value and Allen's theoretical value: (a) for Ag; (b) for Au. The pump laser fluence is set as 0.05 J/m² except for 0.01 J/m² for Au at wavelength of 400 nm. The time step is adopted to be 15 fs except for 6 fs at t_p smaller than 500 fs.

pared to the non-thermalized electrons. When the excitation pulse width is relatively large, electrons are nearly thermalized, and then the extracted e-ph coupling constant in the TTM is slightly underestimated by the influence of non-equilibrium between different phonon branches as shown in Fig. 3 at t_p larger than 900 fs.

The femtosecond pump-probe experiments transform the description of a very complex e-ph energy transfer process into one normalized parameter, which includes not only the electron-phonon interaction, but also the extent of thermal response from electron and phonon temperature changes to reflectance change. For one thing, the excitation pulse width adopted is usually not the actual one irradiated on the metal surface but post-determined,

which may incorporate the effect of e-ph and e-e interaction, even though the e-e scattering is greatly weakened by low fluence excitation [25,40]. For another, the value of a/b which denotes the different extent of thermal response from electrons and phonons might vary by different experimental setup for some metals like Al and Cu [43,44]. More importantly, the different choice of a/b may magnify or weaken the influence of non-thermalized electrons and non-equilibrium between different phonon branches. As a result, the extracted value of the e-ph coupling constant will be affected. Therefore, this study is not intended to compare with experiments directly, which are hard to distinguish the influence of the choice of a/b and t_p or other non-equilibrium effects. In other words, by

performing the quantitative comparison between the BTEs and the TTM, the present work re-examines the extracted e-ph coupling constant in the TTM under the influence of non-thermalized electrons and non-equilibrium between different phonon branches for Ag, Au as a first step.

4. Conclusions

The normalized parameter, which includes electron and phonon temperature changes, is adopted for the direct comparison between the BTEs and the TTM. Through fitting the normalized parameter of the BTEs by that of the TTM, the extracted e-ph coupling constant in TTM is quantitatively re-examined under the influence of the non-equilibrium effects including temporal non-equilibrium between different phonon branches as well as non-thermalized electrons in the present work. The temporal non-equilibrium between different phonon branches will cause the underestimation of the extracted e-ph coupling constant by about 7% for Au, Ag. Moreover, when the excitation pulse width is comparable to the e-ph relaxation time of electrons, the extracted e-ph coupling constant in TTM shows over 20% deviation due to the existence of the non-thermalized electrons. Therefore, if we want to control error within 10%, the excitation pulse width is required to be larger than 300 fs and 500 fs for Au, Ag, respectively at room temperature. This requirement may be easily satisfied in most experiments. The e-e scattering or even electron-photon interaction can be straightforwardly considered for a deeper understanding of the non-thermalized electrons. This work will provide insightful indication for the measurement of the e-ph coupling constant in femtosecond pump-probe experiments.

Declaration of Competing Interest

We declare that there is no conflict of interests for this work.

CRediT authorship contribution statement

Wuli Miao: Investigation, Software, Validation, Investigation, Writing – original draft. **Moran Wang:** Conceptualization, Supervision, Writing – review & editing, Project administration.

Acknowledgements

This work is financially supported by NSF of China (No. U1837602). Our simulations are run on the “Explorer 100” cluster of Tsinghua National Laboratory for Information Science and Technology. The authors appreciate helpful discussions with Y.Y. Guo and G. Yang.

References

- [1] J.M. Ziman, *Electrons and Phonons: the Theory Of Transport Phenomena In Solids*, The Clarendon Press, Oxford, 1960.
- [2] F. Giustino, Electron-phonon interactions from first principles, *Rev. Mod. Phys.* 89 (1) (2017) 015003.
- [3] S.D. Brorson, J.G. Fujimoto, E.P. Ippen, Femtosecond electronic heat-transport dynamics in thin gold films, *Phys. Rev. Lett.* 59 (17) (1987) 1962–1965.
- [4] S. Sullivan, et al., Optical generation and detection of local nonequilibrium phonons in suspended graphene, *Nano Lett.* 17 (3) (2017) 2049–2056.
- [5] S. Anisimov, B. Kapeliovich, T. Perelman, Electron emission from metal surfaces exposed to ultrashort laser pulses, *Zh. Eksp. Teor. Fiz* 66 (2) (1974) 375–377.
- [6] M. Kagnov, I. Lifshitz, M. Tanatarov, Relaxation between electrons and crystalline lattices, *Sov. Phys. JETP* 4 (1957) 173–178.
- [7] P.B. Allen, Theory of thermal relaxation of electrons in metals, *Phys. Rev. Lett.* 59 (13) (1987) 1460–1463.
- [8] R. Bauer, et al., Electron-phonon coupling in the metallic elements Al, Au, Na, and Nb: A first-principles study, *Phys. Rev. B* 57 (18) (1998) 11276.
- [9] A. Jain, A.J.H. McGaughey, Thermal transport by phonons and electrons in aluminum, silver, and gold from first principles, *Phys. Rev. B* 93 (8) (2016) 081206.
- [10] Y. Wang, Z. Lu, X. Ruan, First principles calculation of lattice thermal conductivity of metals considering phonon-phonon and phonon-electron scattering, *J. Appl. Phys.* 119 (22) (2016) 225109.
- [11] Z. Tong, et al., Comprehensive first-principles analysis of phonon thermal conductivity and electron-phonon coupling in different metals, *Phys. Rev. B* 100 (14) (2019) 144306.
- [12] P.M. Norris, et al., Femtosecond pump-probe nondestructive examination of materials, *Rev. Sci. Instrum.* 74 (1) (2003) 400–406.
- [13] G. Eesley, Observation of nonequilibrium electron heating in copper, *Phys. Rev. Lett.* 51 (23) (1983) 2140.
- [14] S. Brorson, et al., Femtosecond room-temperature measurement of the electron-phonon coupling constant γ in metallic superconductors, *Phys. Rev. Lett.* 64 (18) (1990) 2172.
- [15] A.N. Smith, P.M. Norris, Influence of intraband transitions on the electron thermoreflectance response of metals, *Appl. Phys. Lett.* 78 (9) (2001) 1240–1242.
- [16] H.E. Elsayed-Ali, et al., Femtosecond thermorefectivity and thermotransmissivity of polycrystalline and single-crystalline gold films, *Phys. Rev. B* 43 (5) (1991) 4488–4491.
- [17] T. Qiu, C. Tien, Femtosecond laser heating of multi-layer metals—I. Analysis, *Int. J. Heat Mass Transf.* 37 (17) (1994) 2789–2797.
- [18] W. Fann, et al., Electron thermalization in gold, *Phys. Rev. B* 46 (20) (1992) 13592.
- [19] R.H. Groeneveld, R. Sprik, A. Lagendijk, Femtosecond spectroscopy of electron-electron and electron-phonon energy relaxation in Ag and Au, *Phys. Rev. B* 51 (17) (1995) 11433.
- [20] S. Ono, Thermalization in simple metals: Role of electron-phonon and phonon-phonon scattering, *Phys. Rev. B* 97 (5) (2018) 054310.
- [21] M. Obergfell, J. Demsar, Tracking the time evolution of the electron distribution function in copper by femtosecond broadband optical spectroscopy, *Phys. Rev. Lett.* 124 (3) (2020) 037401.
- [22] W. Fann, et al., Direct measurement of nonequilibrium electron-energy distributions in subpicosecond laser-heated gold films, *Phys. Rev. Lett.* 68 (18) (1992) 2834.
- [23] L. Waldecker, et al., Electron-phonon coupling and energy flow in a simple metal beyond the two-temperature approximation, *Phys. Rev. X* 6 (2) (2016) 021003.
- [24] S. Ono, Nonequilibrium phonon dynamics beyond the quasiequilibrium approach, *Phys. Rev. B* 96 (2) (2017) 024301.
- [25] R.H. Groeneveld, R. Sprik, A. Lagendijk, Effect of a nonthermal electron distribution on the electron-phonon energy relaxation process in noble metals, *Phys. Rev. B* 45 (9) (1992) 5079.
- [26] V. Baranov, V. Kabanov, Theory of electronic relaxation in a metal excited by an ultrashort optical pump, *Phys. Rev. B* 89 (12) (2014) 125102.
- [27] W. Miao, et al., Devotional Monte Carlo scheme for thermal and electrical transport in metal nanostructures, *Phys. Rev. B* 99 (20) (2019) 205433.
- [28] B. Rethfeld, et al., Ultrafast dynamics of nonequilibrium electrons in metals under femtosecond laser irradiation, *Phys. Rev. B* 65 (21) (2002) 214303.
- [29] B. Mueller, B. Rethfeld, Relaxation dynamics in laser-excited metals under nonequilibrium conditions, *Phys. Rev. B* 87 (3) (2013) 035139.
- [30] C. Gadermaier, et al., Electron-phonon coupling in high-temperature cuprate superconductors determined from electron relaxation rates, *Phys. Rev. Lett.* 105 (25) (2010) 257001.
- [31] W. Miao, M. Wang, Nonequilibrium effects on the electron-phonon coupling constant in metals, *Phys. Rev. B* 103 (12) (2021) 125412.
- [32] T.M. Tritt, *Thermal Conductivity: Theory, Properties, and Applications*, Springer Science & Business Media, New York, 2005.
- [33] Y. Guo, M. Wang, Heat transport in two-dimensional materials by directly solving the phonon Boltzmann equation under Callaway’s dual relaxation model, *Phys. Rev. B* 96 (13) (2017) 134312.
- [34] X. Ran, M. Wang, Efficiency improvement of discrete-ordinates method for interfacial phonon transport by Gauss-Legendre integral for frequency domain, *J. Comput. Phys.* 399 (2019) 108920.
- [35] T. Qiu, C. Tien, Heat transfer mechanisms during short-pulse laser heating of metals, *J. Heat Transf.* 115 (1993) 835–841.
- [36] Z. Lin, L.V. Zhigilei, V. Celli, Electron-phonon coupling and electron heat capacity of metals under conditions of strong electron-phonon nonequilibrium, *Phys. Rev. B* 77 (7) (2008) 075133.
- [37] T. Qiu, C. Tien, Short-pulse laser heating on metals, *Int. J. Heat Mass Transfer* 35 (3) (1992) 719–726.
- [38] H. Orlande, M. Özisik, D. Tzou, Inverse analysis for estimating the electron-phonon coupling factor in thin metal films, *J. Appl. Phys.* 78 (3) (1995) 1843–1849.
- [39] M. Bass, *Handbook of Optics*, volume IV: Optical Properties of Materials, Non-linear Optics, Quantum Optics, McGraw-Hill, New York, 2009.
- [40] P.E. Hopkins, et al., Boundary scattering effects during electron thermalization in nanoporous gold, *J. Appl. Phys.* 109 (1) (2011) 013524.
- [41] A. Majumdar, P. Reddy, Role of electron-phonon coupling in thermal conductance of metal-nonmetal interfaces, *Appl. Phys. Lett.* 84 (23) (2004) 4768–4770.
- [42] S. Sadasivam, et al., Thermal transport across metal silicide-silicon interfaces: First-principles calculations and Green’s function transport simulations, *Phys. Rev. B* 95 (8) (2017) 085310.
- [43] J.L. Hostetler, et al., Measurement of the electron-phonon coupling factor dependence on film thickness and grain size in Au, Cr, and Al, *Appl. Opt.* 38 (16) (1999) 3614–3620.
- [44] Y.P. Timalisina, et al., Evidence of enhanced electron-phonon coupling in ultra-thin epitaxial copper films, *Appl. Phys. Lett.* 103 (19) (2013) 191602.